

Exact Solutions for the Electromagnetic Fields of a Flying Focus

D. Ramsey,¹ A. Di Piazza,² M. Formanek,³ P. Franke,¹ D. H. Froula,¹ B. Malaca,⁴ W. B. Mori,⁵ J. R. Pierce,⁵ T. T. Simpson,¹
J. Vieira,⁴ M. Vranic,⁴ K. Weichman,¹ and J. P. Palastro¹

¹Laboratory for Laser Energetics, University of Rochester

²Max-Planck-Institut für Kernphysik

³ELI-Beamlines, Institute of Physics of Czech Academy of Sciences

⁴GoLP/Instituto de Plasmas e Fusão Nuclear, Instituto Superior Técnico, Universidade de Lisboa

⁵University of California Los Angeles

All focused laser fields exhibit a moving focus in some frame of reference. In the laboratory frame, an ideal lens focuses every frequency, temporal slice, and annulus of a laser pulse to the same location. The pulse moves through the focus at its group velocity and diffracts over a Rayleigh range. In any other Lorentz frame, the focus moves. “Flying-focus” techniques recreate these moving foci in the laboratory frame by modifying the focal time and location of each frequency, temporal slice, or annulus of a pulse. The intensity peak formed by the moving focus can travel at any arbitrary velocity while maintaining a near-constant profile over many Rayleigh ranges. All of these features make the flying focus an ideal spatiotemporal pulse-shaping technique to enhance a vast array of laser-based applications.

Assessing the extent to which a flying focus can enable or enhance these applications requires an accurate description of the electromagnetic fields. With the exception of the special case $v_I = -c$, all of the aforementioned applications were modeled using approximate solutions for the electromagnetic fields of flying-focus pulses. In the case of conventional pulses with stationary foci, improving the accuracy of approximate solutions has been found to impact models of phenomena ranging from direct laser acceleration to optical trapping. Methods for obtaining accurate solutions to Maxwell’s equations for conventional laser pulses come in three forms: a “Lax”-like series expansion in which corrections to paraxial fields can be calculated recursively; a series expansions of exact spectral integrals for each field component; and the complex source-point method (CSPM), which exploits the invariance of Maxwell’s equations under a translation in the complex plane to transform multipole solutions into beam-like solutions. Of these three, the CSPM is unique in its ability to provide closed-form solutions that exactly satisfy Maxwell’s equations.¹ As a result, the solutions can be Lorentz transformed without introducing additional error.

In this summary, we derive exact solutions to Maxwell’s equations for the electromagnetic fields of a constant-velocity flying-focus pulse. Figure 1 illustrates a schematic of the theoretical approach. The approach combines the CSPM with a Lorentz transformation from a frame in which the focus is stationary to a frame in which the focus is moving. The vector solutions are inherently non-paraxial, can have arbitrary polarization, and are generalized to higher-order radial and orbital angular momentum modes. Subluminal ($|v_I| < c$) and superluminal ($|v_I| > c$) solutions are constructed from multipole spherical and hyperbolic wave solutions, respectively. Propagating the fields backward in space reveals that each solution corresponds to a pulse that was focused by a lens with a time-dependent focal length. Thus, these solutions can be experimentally realized using the flying-focus X (Ref. 2). For a wide range of parameters, the differences between the exact solutions and simpler paraxial solutions are small, justifying the use of paraxial solutions for theoretical or computational studies of flying-focus applications in many regimes.

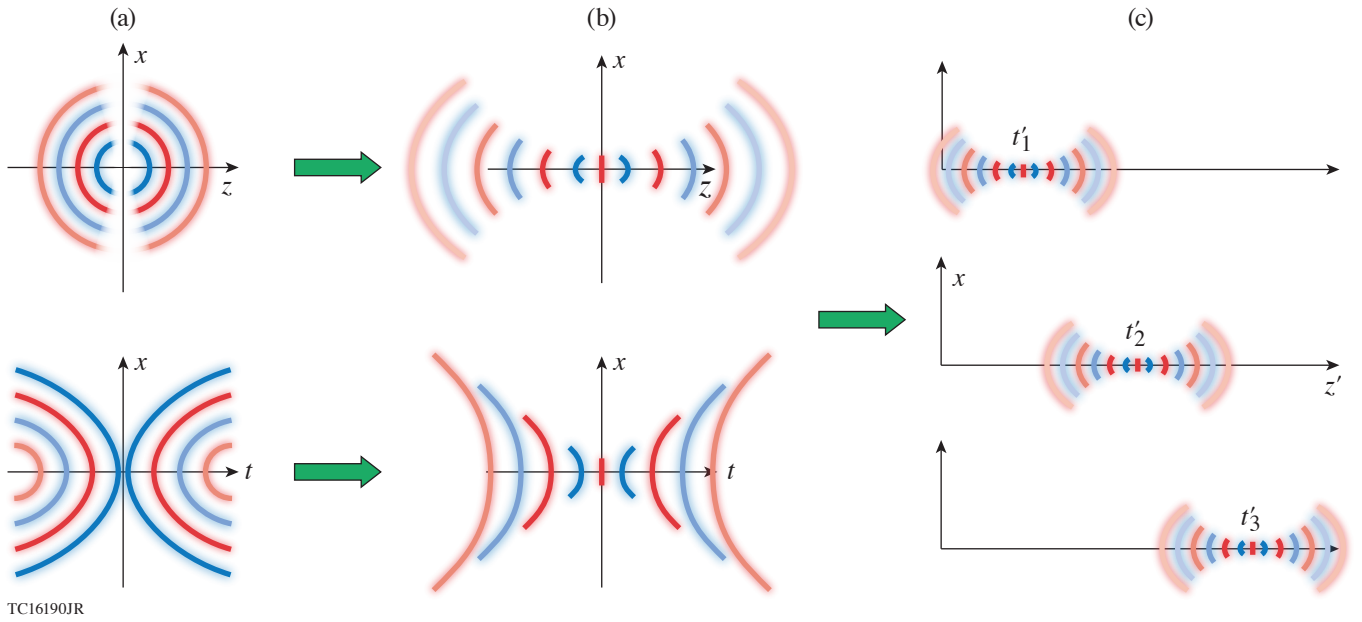


Figure 1

A schematic of the theoretical approach. (a) The approach starts with a multipole spherical (top) or hyperbolic (bottom) solution. (b) A displacement of the coordinate z (top) or t (bottom) into its complex plane transforms the multipole solution into a beam-like solution with a stationary focus in space (top) or time (bottom). (c) A Lorentz transformation of either beam-like solution from a frame of reference in which the foci appear stationary to the laboratory frame produces the exact electromagnetic fields of a flying focus.

As an example, the lowest-order mode electromagnetic fields with polarization vector $\hat{\mathbf{x}}$ are generated by the electric Hertz vector

$$\mathbf{\Pi}_e(\mathbf{x}, t) = \frac{1}{2} \alpha_{00} j_0(\omega R/c) e^{i\omega t} \hat{\mathbf{x}} + \text{c.c.} \quad (1)$$

and magnetic Hertz $\mathbf{\Pi}_m = \hat{\mathbf{z}} \times \mathbf{\Pi}_e$ [Fig. 1(a)], where ω is the angular frequency and α_{00} is an arbitrary constant. After computing the corresponding four potential, the coordinate R is translated into the complex domain as $R \rightarrow \sqrt{x^2 + y^2 + (z - iZ_R)^2}$, where Z_R is the Rayleigh range of the resulting beam-like solution [Fig. 1(b)]. Finally, a Lorentz boost in the axial direction results in a flying focus [Fig. 1(c)]. All of these operations preserve the resulting electromagnetic fields as solutions to Maxwell's equations.

Figures 2(a)–2(f) display cross sections of the resulting electric and magnetic fields at the location of the moving focus $z' = v t'$ for $v_I = 0.5c$ and $\omega w_0/c = 20$, where the primed terms are as observed in the laboratory frame and w_0 is the spot size at focus. The predominant electric and magnetic fields, E'_x and B'_y have equal amplitudes and Gaussian-like transverse profiles. The remaining vector components exhibit more-complex spatial structure, but are much smaller in amplitude. Figure 2(g) illustrates the motion of the focus in the laboratory frame. The cycle-averaged longitudinal component of the Poynting vector $S'_z = c \hat{\mathbf{z}} \cdot \mathbf{E}' \times \mathbf{B}'/4\pi$ is plotted as a function of z' and t' at $x = y = 0$. For comparison, the dashed black line demarcates the speed of light trajectory $z' = ct'$.

This material is based upon work supported by the Office of Fusion Energy Sciences under Award Number DE-SC0019135 and DE-SC00215057, the Department of Energy National Nuclear Security Administration under Award Number DE-NA0003856, the University of Rochester, and the New York State Energy Research and Development Authority.

1. A. L. Cullen and P. K. Yu, Proc. Roy. Soc. A **366**, 155 (1979).
2. T. T. Simpson *et al.*, Opt. Express **30**, 9878 (2022).

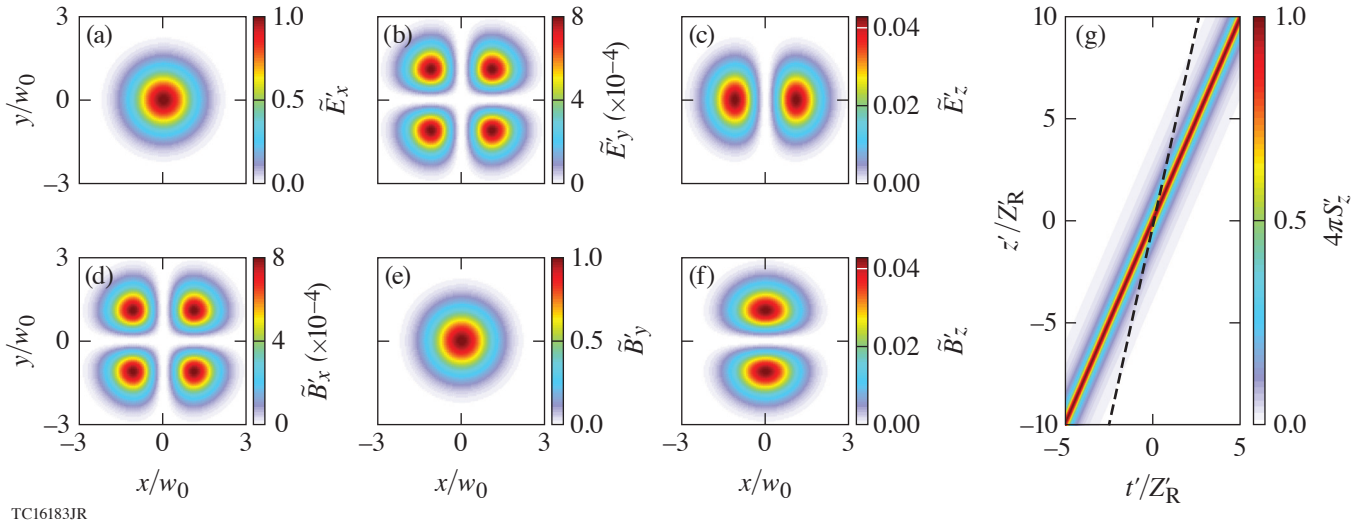


Figure 2

The lowest mode subluminal focus with $v_f = 0.5c$ and $\kappa'w_0 = 20$. [(a)–(f)] Cross sections of the electromagnetic-field amplitudes at the location of the moving focus $z' = v_f t'$. Here $\tilde{E}' = \langle E'^2 \rangle^{1/2}$, where $\langle \rangle$ denotes a cycle average. The amplitudes are normalized to the (\tilde{E}'_x) . (g) The longitudinal component of the cycle-averaged Poynting vector S'_z at $x = y = 0$, showing the motion of the focus. The dashed black line demarcates the trajectory $z' = ct'$ for reference.